EXPERIMENTAL VERIFICATION OF INTEGRATED OPTO-STRUCTURAL MODEL PREDICTIONS

Marie B. LEVINE, Mark H. MILMAN, James W. MELODY

Jet Propulsion Laboratory, California Institute of Technology
Science and Technology Section, Interferometry Technology Program
4800 Oak Grove Drive, Pasadena, California 91109, U.S.A.

ABSTRACT - The JPL Micro-Precision Interferometer (MPI) is a testbed for studying the use of control-structure interaction and vibration isolation technology in the design of precision space-based interferometry. A layered optical control and vibration isolation architecture will be used to achieve the interferometer system requirements in the nanometer range. An important aspect of designing, predicting and implementing the optical control and disturbance compensation schemes for such a system is the need for high fidelity, test-verified analytical structural models. This paper focuses on the new approach implemented to achieve a high-fidelity model for the MPI structure. Pre-test analysis, modal testing, and model updating are summarized for a series of tests at both the component and full system levels. Examples of optical predictions from structural models will be presented.

1. INTRODUCTION

The high precision requirements on the stability, pointing and measurement accuracy of future space interferometry missions will pose great challenges for analysis and modeling research. In particular, the high imaging resolution of future interferometry space missions will require a 10nm *RMS* control of the optical path length over a 10m baseline structure. Hence, these complex missions will require new strategies to integrate structural, thermal, optical and control parameters into unified models of large flexible space structures. Furthermore, these integrated models need to be so accurate as to predict low gravity broad-band nanometer-level optical responses due to micro-g dynamic disturbances and mini-Kelvin temperature fluctuations. These concerns are especially critical for problems involving optical performance prediction, vibration suppression, sensor and actuator placement and structural optimization, Tools are being developed at the Jet Propulsion Laboratory (JPL) in support of high fidelity predictive modeling of opto-mechanical systems. At the core of this effort is the Integrated Modeling of Optical Systems (IMOS) a Matlab-based software which integrates structural, control, optical, and thermal capabilities into a single working environment [MIL97].

More specifically, a methodology is proposed for testing, modal identification and model correlation of complex structures which are assembled in an evolutionary manner. The methodology prescribes initial testing of a base structure without any attached components. The physical properties of the base structure FEM model are updated from the experimental modal properties using a Bayesian Estimation Technique (BET) [LEV92]. The BET is implemented in

MATLAB using IMOS functions, As components are added onto the base structure, additional tests are performed, A testing and analysis approach is proposed which enables estimation of the physical parameters of the components alone. Furthermore, improvements to the original BET implementation have been made which contribute to higher fidelity models and more efficient computational times. These improvements include: a model reduction option based on Component Mode Synthesis (CMS) to increase the computational efficiency of the BET; a Line Search Algorithm (LSA) which accelerates the convergence of the BET; a modal expansion technique which can expand the test mode shapes to the model degrees of freedom, but to a higher accuracy than predicted by the model; and an error localization technique based on element modal strain energy errors (EMSEE) which can locate those elements within the model which are the most inaccurate, either because of deficient model form or of incorrect parameter values.

The paper will discuss in more detail the approach and benefits of using the new mode shape expansion and model error localization. It will then be shown how these new methods were combined with global and component modal testing and identification to achieve an accurate structural model. Experiments conducted on the JPL 7m x 6.3m x 5 .5m Micro-Precision Interferometer (MPI) Testbed Bare-Truss and Phase II configurations are used to evaluate the accuracy of the predictive models. Optics are then incorporated into the improved IMOS structural model, The accuracy of the integrated opto-mechanical model of the MPI testbed will then be demonstrated by comparing open-loop optical prediction to on-board disturbances, such as reaction wheels, with actual experimental measurements.

2. MODEL UPDATING STRATEGY FOR EVOLUTIONARY STRUCTURES

2*1. In-Situ Component Testing

Typically, budget and time constraints do not allow to test the components separately prior to the integration to complex opto-mechanical structures. An in-situ testing approach is proposed in which the components are tested in their integrated configuration on the MPI. In the in-situ component tests the components remain attached to the main structure, but the component response cannot be isolated from that of the main structure. The in-situ component test is conducted in the identical manner as a standard modal test using FRF measurements. Accelerometers are distributed throughout the main structure and the components, and multiple excitation locations can be used, The modes that are identified are those of the coupled component/structure system, In the model updating phase, it is assumed that the FE parameters of the base structure are correct, and that only the FE parameters of the components are uncertain. Sensitivity methods can be used to update the physical parameters of the FE model.

Experimentally, the number of frequency response functions (FRFs) measured for the in-situ component tests is much larger than those required for the other test options, since detailed information of both the component and the structure is necessary to properly identify the modal behavior of the coupled system. Hence, the modal identification and the parameter estimation algorithm with the in-situ component test may become computationally intensive since many FRF measurements are used in the modal identification phase, and because the FEM model must include both the main structure and the components. The computational size can be decreased by using a model reduction technique in the parameter estimation algorithm.

2.2* FEM Model Updating Approach

The standard process for obtaining a high fidelity model of a structure is to perform dynamic tests, to extract the measured modal parameters, and to then improve the FEM model so as to reduce the error between the measured and the analytical dynamic properties. The largest source of error in

this process is in the last step, which is also known as model updating. Model updating techniques fall into two broad categories. Optimal methods use linear optimization methods to change the coefficients in the already assembled FEM mass and/or stiffness matrices, Sensitivity methods apply non-linear optimization schemes to change the physical parameters, such as material and geometric properties, used in the assembly of the FEM mass and stiffness matrices,

A comparative study of many optimal model updating methods performed at JPL has shown that optimal methods are more computationally efficient, but does not always lead to physically realizable systems since the positive definite properties of the mass and stiffness matrix can not be enforced [PEC96].

Although sensitivity methods, such as BET, always lead to physically realizable systems, these methods are very computationally intensive because of the large number of physical parameters needed to form the FEM model, Sensitivity methods also suffer from numerical problems such as convergence to a local minimum, and non-unique trade-offs between the optimized physical parameters. These short-comings can be compensated by reducing the number of physical parameters that are simultaneously updated. This is accomplished by performing phased tests on the structure as components are being added, and by devising a strategy which would allow to detect from the measured data which areas in the model are most likely to be responsible for the errors. In the MPI application, a full modal test was performed on the bare structure to accurately model the truss only. In Phase II, when optical components had been added to the bare-truss, a second modal test was performed, and only the parameters of the new component model were updated under the assumption that the base model was correct. The results are explained in more detail in a later section.

The current numerical implementation of the BET has also been improved by the addition of a line search algorithm which allows for faster convergence to a minimum, and by incorporating a component mode synthesis algorithm to reduce the model to only those components which are being updated, Furthermore, sensitivity methods can only improve on the value of the physical parameters for a defined model form. Examples of model form errors include using the wrong type of element to describe the physical behavior (e.g., rod elements instead of beam elements), or assigning the wrong boundary conditions or nodal constraints. Hence, model error localization schemes should be able to locate both model form errors and physical parameter value errors, It has been concluded that the best approach is to expand the mode shapes and to compare the errors at the model element level.

2.3. Bayesian Estimation Technique (BET)

The sensitivity method selected for the MPI model updating effort is the Bayesian Estimation Technique described in [LEV92] and originally developed by Hasselman et *al.* [HAL91] as the computer code Structural System Identification (S SID). BET is a generalized least-squares estimation method which uses statistical information (*i.* e., the covariance matrix *S*) to weigh the parameters of the objective function, BET uses a linearized approximation of the relationship between the structural parameters and the modal response parameters. The cost functional, *J, is* the weighted sum of the residuals of the test and model eigenvalues, λ, and the difference between the ith estimated parameters, r_i, from their original estimate, r_0 :

$$J = (r_i - r_0)^T \cdot [S_{rr}]^{-1} \cdot (r_i - r_0) + (\lambda_{test} - \lambda_{model})^T \cdot [S_{\lambda\lambda}]^{-1} \cdot (\lambda_{test} - \lambda_{model}) \qquad \text{Eq. 2-1}$$

The first term in the cost fictional is necessary to keep the problem well behaved, essentially requiring the estimated parameters to stay near the original estimate.

The BET used in SSID was modified to include an LSA for more efficient choice of step size. In other words, the BET was used to determine a descent direction:

$$n = \left\| \left\{ [S_{rr}]^{-1} + \frac{\partial \lambda}{\partial r}^{T} , [S_{\lambda\lambda}]^{-1} \cdot \frac{\partial \lambda}{\partial r} \right\}^{-1} \left\{ [S_{rr}]^{-1} , (r_i - r_0) + \frac{\partial \lambda}{\partial r}^{T} \cdot [sA,]^{-1} , (\lambda_{test} - \lambda_{model}) \right\} \right\|_2 \qquad \text{Eq. 2-2}$$

and this descent direction was then passed to an LSA that determined the optimal step size, σ. The LSA used was that of Fletcher [FLE87]. The algorithm essentially brackets the step size and successively moves the brackets together until an acceptable step size is reached. The physical parameters were then updated according to:

$$r_{i+1} = r_i + \sigma \cdot n \qquad \text{Eq. 2-3}$$

2.4. Component Mode Synthesis Estimation (CMS) Algorithm

To reduce the size of the model to be updated, the estimation algorithm was implemented using a CMS Technique, initially proposed by Hurty [HUR64], and later improved by Craig [CRA8 1]. The algorithm is illustrated in Fig. 1. The CMS technique is used to remove from the estimation loop the portion of the model not sensitive to the parameters being updated *(i.e.*, the main structure). Essentially, a model of the main structure is built, solved, and truncated (according to modal frequency) before beginning the estimation loop. The component model is built inside the estimation algorithm loop, as it depends on the estimated parameter, The truncated main structure model is synthesized with the component model in the algorithm loop and solved for the fill modes and mode shapes. From these eigenproperties, and the "mass and stiffness sensitivities, the eigenproperty sensitivities are calculated, With the synthesized eigenproperties, eigenproperty sensitivities, and the expanded test eigenproperties, the descent direction and the step size are found, resulting in an update of the estimated parameter.

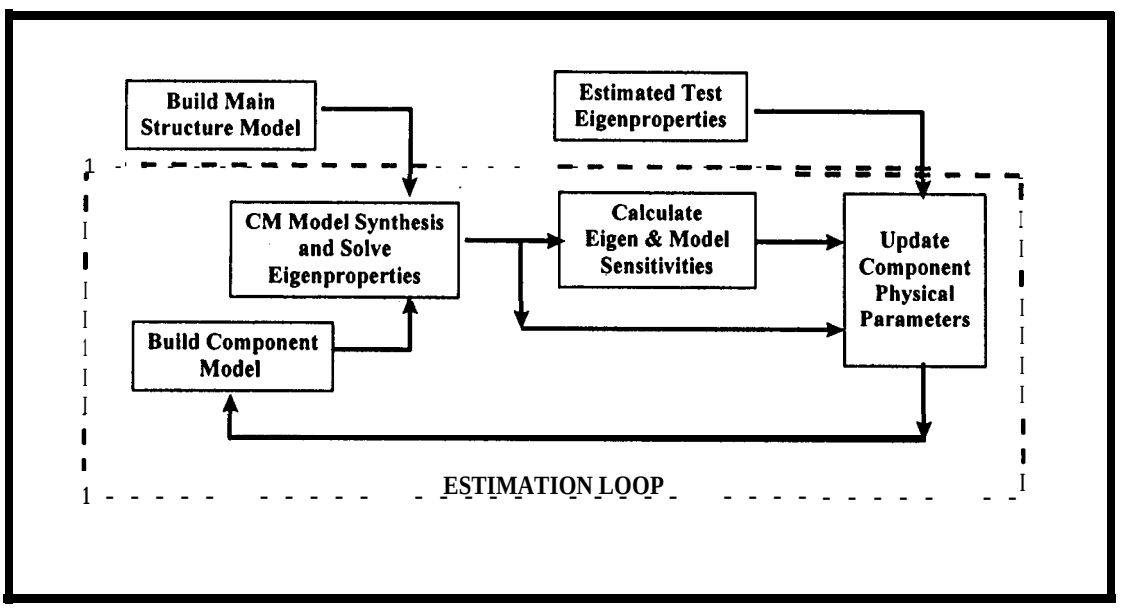

Figure 2-1 Parameter Estimation Algorithm Implemented with Component Mode Synthesis Technique.

2.5. Mode Shape Expansion Techniques

Physical and financial constraints typically limit the number of degrees of freedom (dofs) monitored during a dynamic structural test. These limitations include laboratory or field restrictions, such as available number of accelerometers and/or data channels, structural constraints, such as

inaccessibility of certain parts of the structure, or flight project constraints for on-orbit identification. However, it is often desired to assess the modal response of the full structure at all its dofs. The most common and least demanding reason is for mode shape visualization, Other reasons include correlation of test and analysis results at all the dofs represented in the full Finite Element Method (FEM) model of the structure, As stated above, model updating techniques would benefit from the added information provided by mode shape at all dofs. The full mode shape is also useful in predicting the response at unmeasured dofs for structural integrity and reliability assessments to dynamic loads such as earthquakes, impacts or explosions. Control needs include computation of the strain energy distributions for optimal darnper and active member placement in vibration attenuation problems. In addition, the tuning of Multiple Input/ Multiple Output (MIMO) control parameters and gains also requires an accurate model at all dofs.

Several methods for mode shape expansion have been investigated [LEV96]. The most popular methods use an *a-priori* structural or modal model together with the equations of motions to obtain either a direct solution or an orthogonal projection. Each approach can also be formulated as constrained optimization problems. To account for uncertainties in the measurements and in the prediction, a new expansion technique based on least squares minimization with quadratic inequality constraints (LSQI) has been proposed.

Each modal expansion technique has been fully evaluated with experimental data obtained on the Micro-Precision Interferometer testbed, using both the pre-test and updated analytical models. The studies involve taking a subset of the actual set of instrumented dofs, and verifying the accuracy of the expanded prediction. The robustness of these methods has been verified with respect to measurement noise and model error, It has been shown that the proposed LSQI method has the best performance and can reliably predict mode shapes, and can be used to locate damage elements, even in very adverse situations. A new LSQI algorithm has since been developed which significantly decreases the solution time and the computational requirements of the expansion process [LEV97].

A summary of the findings is presented herein, In the following derivation, "~" refers to experimental data, "--" is the expanded solution, *"a" is the* set of measured dofs, "o" is the set of omitted dofs, and *"f"* is the full set of dofs in the analytical model such that $f = a + o$. *The* four expansion approaches investigated for their accuracy and robustness using actual MPI measurements are the Guyan expansion, the Kidder expansion, the Procrustes expansion, and the new LSQI expansion.

The Guyan or static expansion, based on the Guyan reduction method, assumes that the inertial forces acting on the non-measured dofs can be neglected with respect to the elastic forces [GUY65]. This leads to an exact analytical relationship between the mode shapes at the measured and unmeasured dofs. Using the experimental mode shape data obtained at the instrumented dofs, $\tilde{\phi}_{ai}$, the predicted mode shapes at the full set of dofs, $\bar{\phi}_{fi}$, for the i^{th} mode can thus be inferred from:

$$\bar{\phi}_{fi} = \begin{pmatrix} \tilde{\phi}_{ai} \\ -K_{oo}^{-1} K_{oa} \tilde{\phi}_{ai} \end{pmatrix} \qquad \text{Eq. 2-4}$$

where $\bar{\phi}_{fi}$ is partitioned into measured $\bar{\phi}_{ai}$ and unmeasured dofs $\bar{\phi}_{oi}$. Alternatively, the equivalent constrained minimization problem finds the expanded mode shape $\bar{\phi}_{fi}$ which minimizes the total strain energy of mode *i,* such that the predicted mode shape equals the test values at the measured dofs.:

$$min_{\bar{\phi}_{fi}}\left[\ \frac{1}{2}\bar{\phi}_{fi}^{T} K_{ff}\,\bar{\phi}_{fi}\ \right] \qquad subject \quad \bar{\phi}_{ai} = \tilde{\phi}_{ai} \qquad \text{Eq. 2-5}$$

Equations 2-4 and 2-5 yield identical solutions [LEV97]. However, Eq. 2-4 only requires one matrix inversion, where as Eq. 2-5 requires two, Eq. 2-4 is thus preferred for its computational efficiency.

The Kidder expansion method is based on the dynamic reduction proposed by Kidder [KID73]. The inertial forces are no longer assumed to be negligible, leading to an exact solution of the mode shapes at the unmeasured dofs, ϕ_{oi}, as a function of the test modal frequency, $\tilde{\omega}_i$, and the test mode shapes at the measured dofs, ϕ_{ai}:

$$\bar{\phi}_{fi} \cdot \tilde{\phi}_{ai} \qquad \text{Eq. 2-6}$$
$$[\mathbf{Km} - \tilde{\omega}_i^2\ M_{oo}]^{-1}\ [K_{oa} - \tilde{\omega}_i^2\ M_{oa}]\ \tilde{\phi}_{ai})$$

Similar to Eq. 2-5, a constrained minimization form inspired from the Kidder method is proposed:

$$min_{\bar{\phi}_{fi}}\left[\ \frac{1}{2}\bar{\phi}_{fi}^{T} K_{ff}\,\bar{\phi}_{fi} - \frac{1}{2}\tilde{\omega}_i^2\,\bar{\phi}_{fi}^{T} M_{ff}\,\bar{\phi}_{fi}\ \right] \quad subject \quad \bar{\phi}_{ai} = \tilde{\phi}_{ai} \qquad \text{Eq. 2-7}$$

However, Eq. 2-6 is preferred since it only involves one inverse and avoids the ill-conditioning problem associated with inverting near-singular matrices for $\tilde{\omega}_i \approx \omega_i$.

Kidder's method is computationally more expensive than the Guyan expansion method, since the dynamic stiffness matrix $(K_{oo} - \omega_i^2 M_{oo})$ must be factorized for each mode *i*. With the Guyan method, the partition matrix K_{oo} is only factored once and can be used to expand any mode shape.

Smith and Beattie propose an expansion method expressed as a constrained least-squares minimization [SM190]. This method expands the experimental mode shapes by orthogonal Procrustes transformation of a set of *p* experimental eigenvectors $\bar{\Phi}_p$ into the space spanned by the set of *p* predicted analytical eigenvectors Φ_p at the measured dofs *a:*

$$min_{P_{pp}}\ \Phi_{ap} - \Phi_{ap}\ P_{pp}\ _2 \quad subject \quad P_{pp}^T\ P_{pp} = I \qquad \text{Eq. 2-8}$$
$$\bar{\Phi}_{fp} = \Phi_{fp} P_{pp}$$

The Procrustes transformation is a mathematical technique which rotates two sets of same dimension into each other, The orthogonal transformation matrix P_{pp} is computed for the *p* experimental and paired analytical mode shapes at the *a* measured dofs through a singular value decomposition. The Procrustes transformation preserves mass orthogonality and is numerically efficient. However, it requires correct pairing between the analytical and experimental eigenvectors, and selection of a set of measurement locations which fully spans the space of the *p* modes used for the expansion. Smith has attempted a variation of the Procrustes orthogonal expansion method which retains the measured degrees-of-freedom (dofs) values and transforms only the unmeasured dofs. This modification was not recommended since it resulted in a loss of orthogonality in the eigenvectors, and a more jagged appearance in the mode shapes (e.g., "loss of smoothing").

Although Procrustes' method is more computationally efficient in expanding mode shapes than the Guyan and Kidder method, it does require the analytical eigenvalue problem to be solved. This may be computationally demanding for large models.

The constrained minimization versions of the Guyan and Kidder expansion methods impose that the value of the expanded mode shape at the measured dofs, $\bar{\phi}_{ai}$, identically equals the measured values $\tilde{\phi}_{ai}$ (Eqs. 2-4 and 2-6). Existing errors in the experimental values propagate errors in the estimates of the mode shape at the unmeasured dofs $\bar{\phi}_{oi}$. Furthermore, ordinary experimental errors may impede optimization problems with equality constraints. When the equality between the measured

data and the optimized data cannot be met *individually at every dofs*, the constrained optimization problem may either have an impossible solution or the wrong solution. Although penalty methods or generalized least-squares methods could be formulated to incorporate uncertainties resulting from experimental or analytical errors, the solution is dependent on the value of the relative weighting parameter S, While S is theoretically related to the covariance of the measurement and model errors, its correct value is difficult to assess,

To bypass these weaknesses, the modal expansion problem can be reformulated as a quadratic minimization with the understanding that error in the expanded mode shape exists, and that it is bounded by the expected measurement error. Mathematically, this is a least-squares minimization problem with quadratic inequality constraints (LSQI) of the general form:

$$min_{\bar{\phi}} \left|A\bar{\phi} - b\right|^2 \ subject \ to \ \left|B\bar{\phi} - d\right|^2 \le a\ \tilde{\phi}\Big|^2 \qquad \text{Eq. 2-9}$$

The immediate advantage of the LSQI formulation is to allow convergence within a domain of probable solutions, while taking into account uncertainties associated with experimental errors.

Several LSQI formulations for mode shape expansion have been proposed and investigated [LEV94]. When tested on actual data, the LSQI counterparts of the constrained optimization form of the Guyan and Kidder methods (Eqs. 2-5 and 2-7) gave answers as accurate as the ones predicted by the direct solutions (Eqs. 2-4 and 2-6), with no computational advantage. Furthermore, it was found that closely matched experimental and modal frequencies resulted in quasi-singularities and ill-conditioning of the objective function.

To circumvent this problem, the objective function is redefined as the quadratic norm of the modal residual force. With this new formulation, the LSQI problem now finds the optimal $\bar{\phi}_{fi}$ which minimizes the modal residual force such that the quadratic error between the expanded mode shape and the experimental mode shape at the measured dofs is within the bounds expected from experimental error.

$$min_{\bar{\phi}_{fi}} \left|\left(K - \tilde{\omega}_i M\right)\bar{\phi}_{fi}\right|^2 \ \ subject \ to \ \left|\bar{\phi}_{ai} - \tilde{\phi}_{ai}\right|^2 \le \alpha\left|\tilde{\phi}_{ai}\right|^2 \qquad \text{Eq. 2-10}$$

As a $\alpha \Rightarrow 0$, LSQI indirectly solves the eigenvalue problem for the given experimental modal frequency and mode shape at the measured dofs.

Mathematical techniques for solving this problem have been published and are easily implemented [GOL83]. However, standard solution techniques for the LSQI method involve a generalized singular value decomposition of the full NxN dynamic force matrix A, and the αxN partitioning matrix B, which require $O(N^3)$ operations. This can become prohibitively large when expanding modes of structures with over 1000 dofs. A new LSQI algorithm is proposed, which takes advantage of the fact that the number of measured dofs, a, is much less than the number of dofs in the model [LEV97]. It is shown that this new method simultaneously diagonalizes matrices A and B as the sum of two orthogonal projections. The improved algorithm requires $O(Na+a^2)$ operations, and is made even more efficient by using a sparse matrix formulation. When applied to the test data expanded from 408 to 1573 dofs, the computational time on a Sun Sparcstation 10 was reduced from 3 days to 1 hour,

2.6. Mode Shape Expansion Validation

2.6.1. Performance Metrics

To assess the error between the expanded and actual mode shapes a first error metric is proposed which evaluates the relative quadratic point-to-point error at all dofs f between the predicted expanded mode shape ϕ_{fi} and the actual measured mode shape ϕ_{fi} for each mode *i:*

$$\Delta(i) = \frac{\bar{\phi}_{fi} - \tilde{\phi}_{fi}}{|\phi_{fi}|} \qquad \text{Eq. 2-11}$$

In comparing mode shapes at each point, normalization of the eigenvectors is achieved by least squares fit of the expanded mode shape to the reference mode shape. Alternatively, the mean cumulative error in the mode shape as a function of the mode n can be used to determine the modal number at which the expansion methods start to break down :

$$\varepsilon(n) = \frac{1}{n} \sum_{i=1}^{n} \Delta(i) \qquad \text{Eq. 2-12}$$

The orthogonality properties of eigenvectors, as inferred in the Modal Assurance Criteria (MAC), can also be used as a performance metric. The MAC matrix between the expanded and analytical eigenvectors is defined as:

$$MAC_{ij} = \frac{\left|\bar{\phi}_{fi}^{T} \cdot \phi_{fi}\right|}{|\phi_{fi}|} \qquad \text{Eq. 2-13}$$

The MAC is used to verify the orthogonality between the expanded mode shapes and the actual mode shapes measured at all dofs. The mass cross-orthogonality condition (MX) is also a potential performance metric. However, when applied to this case study, MX provided the same information as the MAC. Both the MAC and the MX are widely used model correlation indexes in the aerospace trade.

It is relatively straightforward to establish that the MAC (Eq. 2-13) is proportional to the square of the normalized difference between eigenvectors (Eq. 2-11). For example, a norm difference of 10% between two eigenvectors is equivalent to a MAC of approximately 0.99. Thus the norm error is a significantly more sensitive measure of performance than the MAC, and will be used in the following experimental evaluation.

2.6,2. Performance to Ideal Measurement and Updated Model

The performances of the Guyan method, the Kidder method, the Procrustes method and the LSQI method have been extensively evaluated with respect to measurement error, model error, and measurement location [LEV96]. Only the most significant results are presented herein. The expansion is performed from a subset of the 240 dofs measured during the dynamic tests, A particular set of instrument location is referred to as "*aset5*". It contains 12 dofs, the location of which are optimally selected using a modal kinetic energy criteria, *Aset5* provides enough information to identify the first nine modes, with the exception of mode 6 which is not properly represented. The expansion of missing mode 6 will thus provide a measure of the methods' robustness to unmeasured modal information, The 240 dofs locations represent 3 dofs at each of the 80 node balls forming the truss structure. The fill FEM model used for the expansion also has 240 dofs, in which each dof matches a test location, The expanded mode shapes are then compared to the actual experimental values using the cumulative error performance metric for the first nine modes (e.g., $\varepsilon(9)$ in Eq. 2-12).

The expansion methods are first investigated for their reliability and performance when all experimental and analytical conditions are favorable. The expansion is executed with the updated (i.e., "ideal") analytical FEM model and mode shapes, from a subset of the high quality experimental data measured on the MPI. The measured data is not corrupted by additional noise. Here, the twelve *aset5* locations have been retained as the "measured set", and are expanded to the full 240 dofs recorded during the actual test, The error of the ideal analytical model with respect to the full 240 dofs measurement set is also included in Fig. 2-2 for reference. Based on the comparison between two independently performed modal tests, mode shape errors below 15% are acceptable and within

the experimental accuracy of the measurements [LEV94]. The Guyan method can only expand the first 2 modes properly, after which the estimates are unreliable. To get suitable expansion with the Guyan method, a minimum ratio of 3 to 4 accelerometers per mode is required - as commonly practiced experimentally. Lower ratios of instrumented dofs to modes and better performance can be achieved with the Procrustes, the Kidder and the LSQI expansion methods,

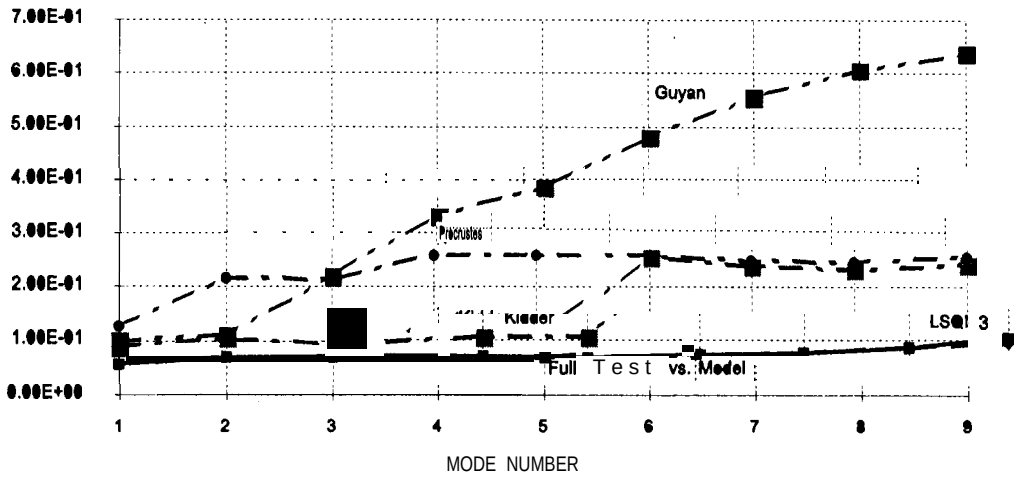

Figure 2-2 Mean cumulative mode shape error -Expansion from 12 dofs(*aset5)* to 240 dofs with updated FEM model and no additional measurement noise.

The Kidder method generates expanded mode shapes which have errors of only 10% for seven of the nine modes, but mode 6 could not be identified, Mode 6 is also the mode which is not captured by the accelerometer location. Hence, under ideal experimental and analytical conditions, the Kidder method can correctly expand all modes measured by the accelerometer location set. The Procrustes expansion method can predict mode 6, but only modes 1 and 3 have acceptable error levels. The mediocre results are explained by the fact that all nine modes are expanded simultaneously from the initial 12 dofs subset. It was observed that the Procrustes method is very sensitive to the number of simultaneously expanded modes and to the set of measurement locations,

The LSQI expansion method performs the best across all modes. It is capable of predicting unmeasured mode 6 better than the Procrustes method, Foremost, it is the only expansion method investigated so far which results in estimates which are as accurate as the full set of measured mode shapes.

2.6,3. Sensitivity to Measurement Error *And* Model Error

There are many sources of noise in the processing of mode shapes: accelerometer accuracy, wire mass and darnping, shaker coupling, method of excitation. An additional error can be introduced by the modal identification method itself, It suffices to say that the measured mode is never pristine, 'It could be desirable, therefore, to have a mode shape extrapolation procedure that is not only insensitive to noise, but that can filter it out too.

For lack of a better model, the measurement noise is represented as an additive random error superimposed upon the true mode shape. Future work should investigate the effect of non-Gaussian measurement errors representative of a defective sensor or a consistent operator error. In the following, an additional 25% error was added to the experimental mode shape data, It is recalled that the 15°A error is the level expected from standard experimental procedures. The mean expansion prediction is inferred by averaging 30 Monte Carlo simulations. The expansion is from *aset5* with 12 dofs up to the full 240 dofs of the model.

The FEM model plays an important role in the regularization of spurious information, the filtering out of the measurement error, and the prediction in the event of insufficient information. This is especially true of the Kidder and the LSQI methods which rely heavily on the fill dynamic equations. In the following, both distributed (i.e., global), and localized errors are investigated,

Distributed errors in the analytical mass or stiffness matrix, such as errors resulting from the uniform structural properties (e.g., mass density or modulus of elasticity), only scale the eigenvalue problem by a multiplicative constant, and have little influence on the modal expansion prediction. Another form of global model error can be introduced by deficiencies in the model form, as would typically occur in a pre-test model. To this effect the actual pre-test model of the MPI is used for demonstration, It is composed uniquely of rod elements, and can only approximately predict the first 4 modes. The "ideal" updated model used in the previous expansion analyses is constructed uniquely of beam elements, and can accurately predict the first nine modes.

Spatially localized model error, such as would occur from local errors in the model form or properties, or from changes in the actual structure resulting from fatigue or damage are also expected to affect the predictability of the expanded mode shapes, To simulate this situation the stiffness of the longest strut in the pre-test model, connecting the tower to the optics boom, is decreased by half. This only changes the pre-test frequencies of modes 5 and 6 by less than 3%, while keeping all other frequencies almost the same, However, the effect of this localized error on the analytical mode shapes is significant, as shown in Fig. 2-3, where a major jump for mode 5 and 6 correspond to a 300% increase in the mode shape error relative to the "undamaged" pre-test model.

The performance of the expansion methods is assessed for the combination of global and local modelling error with an additional 25°/0 error in the measured mode shape values, The results are summarized in Fig. 2-3. The solid lines represent the accuracy of the different forms of the MPI model with respect to the true test data at all dofs, and the dashed lines represent the expanded mode shapes from *aset5* to the full 240 dofs using the damaged pre-test model and noise corrupted measurements.

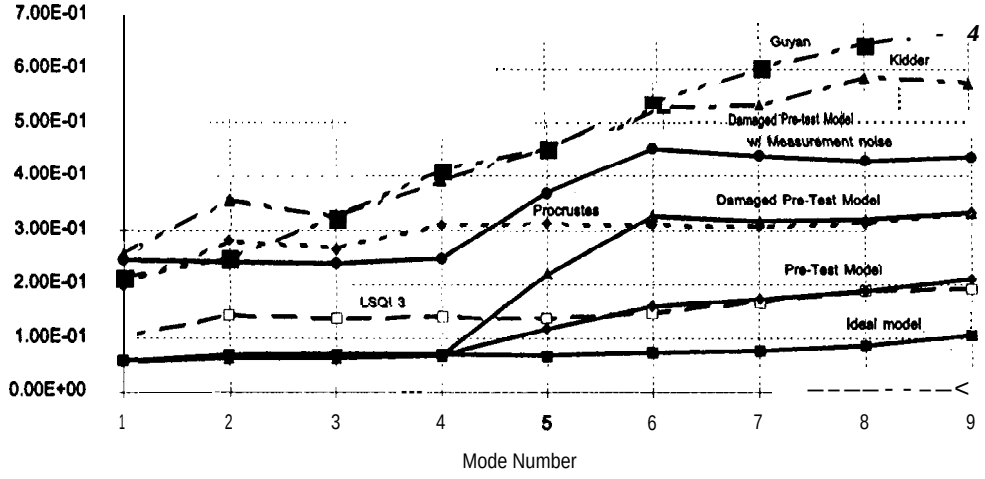

Figure 2-3 Mean cumulative mode shape error - Expansion from 12 dofs *(aset5)* to 240 dofs with damaged pre-test FEM model and 25% additional measurement noise,

As expected, adding measurement noise to the damaged pre-test model significantly worsens the performance of all the expansion methods (Figs, 2-2 and 2-3), In the presence of both model error and measurement noise, the Guyan and the Kidder method perform equally poorly, and generate

mode shapes which are worse than predicted by the damaged pre-test model. The Procrustes method performs better than the Guyan and the Kidder methods, especially at the higher modes, and can predict the lower modes to the same level of accuracy as the noise contaminated data. However, the Procrustes method is very sensitive to measurement dof location and selection, as well as to the number of simultaneously expanded modes, In an actual situation this is a big disadvantage as the real solution is not known, and the variation in the error can be great.

The LSQI method performs exceptionally well. It generates mode shapes which are only off by 15%, although the data used is contaminated by 250/. noise and the model has the wrong form and a damaged member. Only the LSQI method is capable of expanding mode shapes to an equal or greater level of accuracy than the measured data, even when the original data is corrupted by significant amounts of noise. In fact, for moderate amounts of measurement noise, e.g., less than 25%, the first nine modes expanded with the LSQI method from only 12 instrument locations are almost as accurate as the noise-free mode shapes measured at all dofs.

2.7. Model Error Localization Techniques

The error metrics discussed above are global metrics describing the total error throughout the whole set of dofs. Errors can also be evaluated at the local structural element level by the strain energy distribution associated with each element s and with each mode i. Analogous to the mass cross-orthogonality which measures the accuracy of the expanded mode shape with respect to the FEM mass matrix M, the element modal strain energy verifies the fit of the i^{th} expanded mode shape at the dofs of elements with respect to the FEM element stiffness matrix k_{ss}. In the following definition, $\bar{\theta}_i^s$ is the s^{th} element modal strain energy for the expanded mode shape, which is normalized with respect to the total strain energy for the i^{th} mode,

$$\bar{\theta}_i^s = \frac{\left\langle \bar{\phi}_{fi}^s, k_{ss}\bar{\phi}_{fi}^s \right\rangle}{\left\langle \bar{\phi}_{fi}, K\bar{\phi}_{fi} \right\rangle} \qquad \text{Eq. 2-}$$

A large modal strain energy for a particular element and a given mode shape signifies that the element stores a large proportion of-the mode shape's strain energy, Thus, finding those elements in which the differences between the measured and the analytical element modal strain energies are the largest provides a systematic criteria for the selection of the elements most responsible for the model error. The element modal strain energy error (EMSEE) between the analytical θ_i^s and the expanded $\bar{\theta}_i^s$ identifies the discrete dofs where the expansion does not agree with the model. Such errors typically result from localized modelling errors or actual structural damage,

EMSEE calculation uses IMOS FEM capabilities to estimate modal strain energies in rod, beam or plate elements. EMSEE also takes into account model reductions from IMOS rigid body elements (RBE). For a single MPI mode shape (1573 independent dofs), EMSEE calculations for all elements require 15 minutes on a Sun Sparcstation 2.

The mode shapes expanded with the Guyan, Kidder, Procrustes and LSQI method are compared for their capability to locate darnaged or ill-modeled elements. The error localization criterion is implemented on the "damaged" model described above. For the purpose of this analysis, the measured test data contains the *true* information about the state of the structure, and the model includes a localized error in one of its members. The element whose stiffness is decreased by half is labeled #167 in the finite element model. The measured mode shapes describing the *true* state of the structure are expanded from *aset5* (12 dofs) up to the full 240 dofs using the "damaged" model, for the Guyan, Kidder, Procrustes and LSQI methods. The element modal strain energies (Eq. 2-14) are then computed for both the expanded mode shapes and the analytical mode shapes predicted by the "damaged" model using the darnaged element stiffness matrix k_{ss}. *The* two element strain energies

are then compared for each mode *i*. *The* damaged or ill-modeled elements are those that have the highest discrepancy between the analytical and the experimental modal strain energies.

The results are listed in Table 2-1, in which the correctly identified element has been shaded out. The first column lists the ideal case where the element modal strain energies of the undamaged model is compared to those of the damaged model, For 8 out of the 9 modes, element#167 has been correctly identified as the damaged element, proving that the element modal strain energy is an appropriate error identification criterion. The damaged element was not identified at all with the Guyan expanded mode shape, and only once with the Kidder and Procrustes expanded mode shapes, However, the LSQI expanded mode shape accurately identified the damaged element in 4 out of the 9 modes. Thus, the LSQI mode shape expansion method is also the most appropriate expansion technique for identifying damaged members or localized model error, even in the presence of measurement noise.

MODE #	*UNDAMAGED MODEL*	*GUYAN*	*KIDDER*	*PROCRUSTES*	*LSQI*
1	[redacted]	124	18	26	124
2	[redacted]	15	137	55	168
3	[redacted]	137	120	109	137
4	[redacted]	38	124	109	[redacted]
5	[redacted]	77	[redacted]	166	[redacted]
6	26	157	62	157	[redacted]
7	[redacted]	217	64	[redacted]	[redacted]
8	[redacted]	217	3	157	137
9	[redacted]	36	210	26	209

Table 2-1. Element numbers with the highest modal strain energy errors relative to the damaged model, The shaded box is damaged element #167 with -50% stiffness.

3. APPLICATION ON THE MPI

The Micro-Precision Interferometer (MPI) testbed at the Jet Propulsion Laboratory (JPL) is a lightly-damped truss-structure comprised of two booms and a vertical tower with dimensions of $7m$ x $6.3m$ x $5.5m$, and weighing210 *kg*. It is composed of 250 aluminum struts connected to 80 node balls. The primary objective of the MPI is to perform system integration of vibration attenuation and optical control technologies to demonstrate the end-to-end operation of a space-based optical interferometer [NEA97]. Accurate modeling and response prediction are essential for the successful implementation of these control methodologies and optical metrology functions.

3.1. MPI FEM Models

Consistent with the proposed strategy, a first modal test and BET model updating effort was performed on the MPI tested in its bare-truss configuration [LEV92]. Also during this effort, individual struts were tested to extract the correct model form and physical properties for the components. It was concluded that to capture the proper bending behavior, each strut needed to be modeled by five individual beam elements. The bare-truss MPI model was accurate for the first 14 flexible body modes (< 60 Hz) and contained over 10,000 dofs. However, the model size needed to be reduced to less than 480 dofs as to allow for the additional models of the optical components. A model reduction scheme was devised such as to find the optimal physical properties of the strut modeled as a single beam element with respect to the first and second bending modes of the high fidelity five-element strut model. This optimization was performed for

each of the twelve different strut assemblies comprising the MPI bare-truss. After performing the element reduction, the 480 dof reduced IMOS MPI bare-truss model was accurate for the first ten flexible body modes up to 50 Hz.

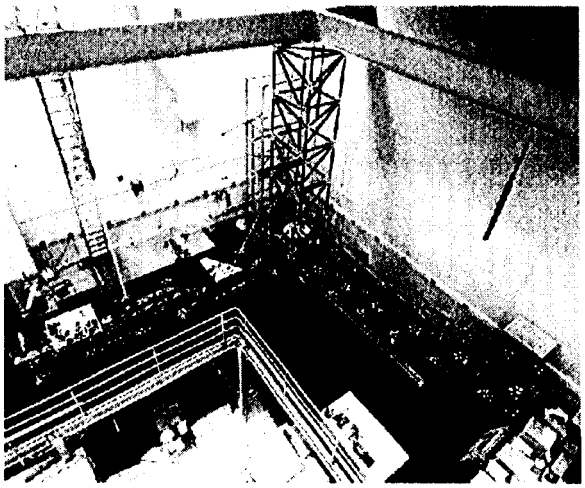

Figure 3-1 Micro-Precision Interferometry (MPI) testbed phase II configuration Finite Element (FE) model.

Just as the MPI Testbed hardware had evolved from Phase I to Phase II of its delivery, so was it necessary to add component models to the FEM model of MPI bare-truss (Fig. 3-1). These components include two optics plates, an active optical delay line and its support structure (a.k.a., trolley), two siderostat mount structures, and a payload plate. The phase 11 model was implemented on a Sun Sparcstation 10 using the IMOS software package, where it could easily be integrated with optical and controls models in the future. Furthermore the Sparcstation and IMOS were both available resources, After the component models were added, the Phase II model had 1973 dofs, of which 1573 were independent dofs.

3.2. MPI In-Situ Testing.

The component models having been added to the bare-truss MPI model, analytical mode shapes and FRFs are predicted for the MPI Phase II configuration. Modal tests were performed on the MPI structure, with its added components using the in-situ component test approach. The tests were performed with a modest suite of test equipment (shaker, accelerometers, and DAS). From the resultant test data, experimental mode shapes were identified at the instrument locations (i. e., test dofs). The LSQI modal expansion technique was applied in order to expand the mode shapes to the model dofs. Estimation of the error between the expanded experimental mode shape and the predicted analytical mode shape using the Element Modal Strain Energy Error (EMSEE) discovered model form errors and provided a selection criteria for determining the physical parameters to be updated.

The Phase 11 MPI was tested in a free-free configuration suspended at 3 points by an assembly of springs and bungee cords, The bungee cords were added to increase the suspension stiffness and to damp out the troublesome suspension surge modes, The in-situ test involved a single shaker location and multiple, roving-accelerometer measurements throughout the MPI, with emphasis on the trolley and plate components.

The shaker used for the experiment was a low-level Bruel and Kjaer l-Newton shaker, attached to the structure by a 10-inch metal stinger, which was itself connected to a Dytran 10-pound load cell. A total of 424 output dofs were recorded using roving micro-g Kistler tri-axial

accelerometers. The tests were controlled with an Hewlett-Packard 6066A 16-channel DAS on a 486 PC host computer. The tests were performed using burst random inputs with a bandwidth of 2 Hz to 102 Hz.

3.3. MPI Modal Identification and Expansion.

Modal identification was performed using SDRC/IDEAS Modal software package on a MicroVAX. The 424 test FRFs were used to identify the modal parameters of the MPI testbed. Various curve-fit options were available in IDEAS, each capable of producing global estimates of modal frequencies, damping, and mode shapes. The Polyreference method was used because it provided a modal confidence factor for each estimated mode, which facilitated the elimination of fictitious computational modes,

The LSQI expansion technique was applied to the first 13 flexible body mode shapes up to 45 Hz. The test mode shapes were expanded from the 408 measured dofs to the 1573 independent dofs of the Phase II MPI model. Expansion of each mode originally took roughly 3 days in IMOS on a Sun Sparcstation 10, The expansion time was reduced to roughly one hour, a 70 to 1 reduction, with the improved LSQI algorithm,

Correlation between the test and analytical mode shape is evaluated with the Mass Cross-Orthogonality (MX). The MX weighs the modal correlation proportionally to the mass contribution at each dof. Correlation between the measured modes and analytically predicted modes for the pre-test model are listed in Table 3-1. Only modes 1, 2 and 5 are properly correlated with MX greater than 90 % and with frequency errors less than 2%.

3.4. MPI Phase II Model Updating

The accuracy of the stages of the Phase II MPI FEM model are shown in Table 3-1. After the new components were added to the model but prior to any adjustment to fit the test data, only the lowest two flexible body modes were modeled accurately (<10Hz). After evaluating the model with the EMSEE, several model form errors were found. These were human errors in modeling of the trolley flexures and the trolley truss elements, and lack of fidelity in the modeling of the trolley flexures. In particular, the flexures supporting the optical delay line had been oriented about the wrong axis. A second model form error was very subtle, yet contributed to inappropriate bending mechanism of the delay line. The pre-test model assumed that the diagonal elements of the delay line had neutral axis about the center of the beam. However, because of the welding of the joints, the neutral axis was in effect shifted, After these model form errors were corrected, significant improvement was made in the accuracy of the model, with four of the lowest five modes being modeled correctly. Of the first five modes, the fourth had an acceptable MX, but a large frequency error of-6.7%.

After implementing the corrections in the model form, EMSEE was applied to select the physical parameters to be updated. The parameters were then estimated using a BET modified by a LSA for faster convergence. CMS was used in order to improve the algorithm's computational efficiency. The EMSEE was applied to the corrected model, and the optical delay line was still responsible for the largest source of error, Due to time and finding limitations, only a single parameter was estimated, The parameter chosen was the trolley truss parameter that significantly affected the fourth flexible body mode. The full Phase 11 MPI model was reduced with the CMS approach down to a single component of the structure, The CMS implementation of the estimation algorithm resulted in a reduction of the size of the eigenvalue solution *inside the loop* from 1573 dofs to 503 dofs, corresponding to a reduction in the solution time from 4 hours to roughly 5 minutes on a Sparcstation 10, The error in the eigenproperties resulting from the modal truncation

of the main structure model was negligible (modal frequency error < 0.010/0, MX > 99.9°/0 on diagonals). The parameter estimation procedure resulted in an accurate representation of the all of the first five flexible body modes (<20 Hz) (Table 3-1).

TEST			PRE-TEST MODEL			CORRECTED M O D E L				ESTIMATED MODEL		
					MX			MX				MX
Mode #	Freq (Hz)	Damp (%)	Freq (Hz)	AF o/o	test dofs	Freq (Hz)	AF o/o	test dofs	full dofs	Freq (Hz)	AF o/o	full dofs
1	6.55	0.41	6.58	0.5	0.98	6.56	0,2	0.97	0.90	6.56	0,1	0.90
2	9.39	0.40	9.25	-1.5	0.99	9,10	-3.1	0.99	1.00	9.10	-3.1	1.00
3	11.5	0.41	11.2	-2.7	0.71	11.4	-0.9	0.97	0.99	11.5	0.1	1.00
4	12.9	0.27	11.6	-11.2	0.69	12.1	-6.7	0.96	0.98	12. 7	-1.5	1.00
5	19.3	0.48	19.7	2,0	0.96	19.2	0,5	0.96	0.95	19.3	-0,2	0.96
6	24.1	0.21	23.9	-08	003	23.3	-34	073	028	233	-34	029
			24.9	3.2	0.24	24,4	1.2	0,62	0.25	24.4	1,2	0.25
7	28.8	0.45				33.5	14.0	0.88	0.49	33.6	14.1	0,49
8	33.8	0.35	35.4	4.5	0.79	34,9	3.2	0,87	0,90	34.9	3.2	0.90
9	36.9	0.41	-	-	-	39.6	6.8	0.87	0.20	39.6	6.8	0.20
10	39.8	0.15	38.4	-3.4	0.77	39.2	-1.5	0.86	0.85	39.2	-1.5	0.85
11	41.8	0.19	40,1	-4.2	0.88	40.4	-3.5	0.84	0.89	40.4	-3.5	0,89
12	43.2	0.22	44.2	2.3	0.61	42,6	-1.4	0,39	0,13	42.6	-1.4	0.14
13	44,7	0.29	46.7	4,3	0.48	46.8	4.5	0,65	-	45.3	1.3	-

Table 3-1: Results of in-situ parameter estimation for the MPI testbed. Modes that showed a significant improvement in accuracy from the previous model are shown in italics.

A graphical representation of the analytical prediction improvement is shown in Fig. 3-2 for the FRF between the shaker input and a response location on the optical delay line component measured during the in-situ component tests, The solid line is the actual measured FRF. Overlaid on the plot are the predicted analytical FRFs from the pre-test uncorrected model, the model corrected for the model form error, and the model which was further improved for physical property value ("estimated model"). Correcting for the model form errors is the largest contributor to improving the match between the measured and analytically predicted FRF. Improving the physical properties for one of the optical components using the BET sensitivity update method, as represented in the "estimated model", further accounts for a small shift in frequency. This demonstrates the importance of identifying model form errors prior to updating physical parameters.

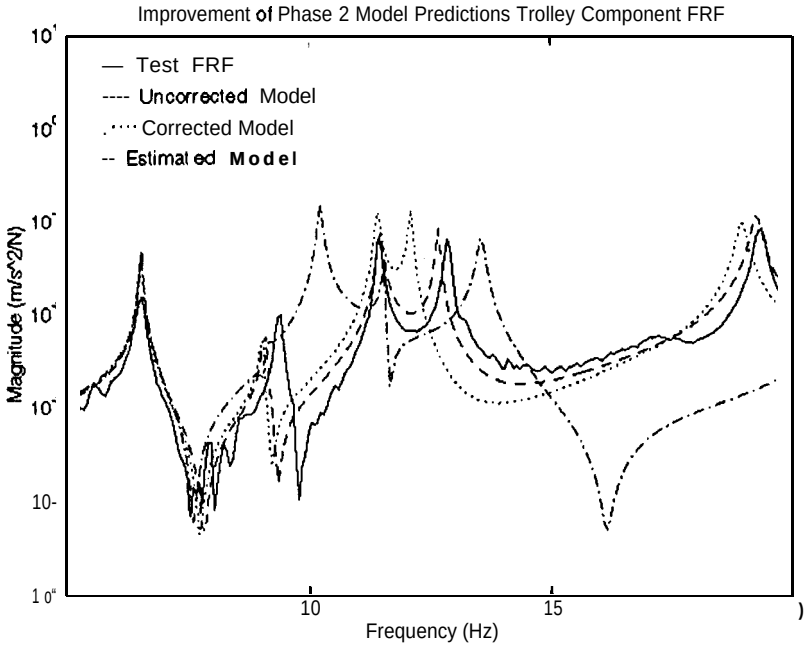

Figure 3-2 Model Prediction Improvement for the Predicted Optical Trolley Component FRF.

4. MPI OPTO-MECHANICAL MODEL VALIDATION

Once the structural model has been updated to match the measured modal properties, optical component models and control systems are added to the IMOS model for a truly integrated opto-mechanical model. Extensive testing has been performed on the MPI Phase 11 configuration to validate the integrated model predictions with actual experimental measurements [NEA97, MEL96]. Disturbances have been applied with a shaker to the actual MPI structure to obtain open-loop and closed-loop fringe position and optical path length difference (OPD) transfer functions. For validation of the analytical predictions, these same transfer functions have also been generated from the integrated MPI model,

As an example, Fig. 4-1 shows the IMOS geometric layout of the open-loop MPI transfer function between an x-axis shaker force to the stellar OPD output, The measured experimental results are shown as the solid line in Fig.4-2. The improvements in the predictions from the pre-test (uncorrected) model, to the corrected model, and to the estimated model are also shown in dashed lines. It is seen that for this particular example, the identified model form errors identified through the LSQI expansion technique and EMSEE criteria are the largest contributor to the improved match between the experimental data and the analytical predictions, Thus, validating IMOS and the analysis approach as a viable tool for high fidelity predictive modeling.

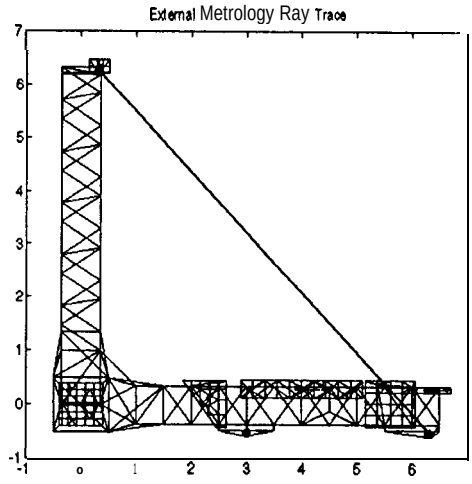

Figure 4-1 IMOS Geometric Configuration of the MPI Phase II for External Metrology Transfer Function Prediction to Dirty Box Input Force.

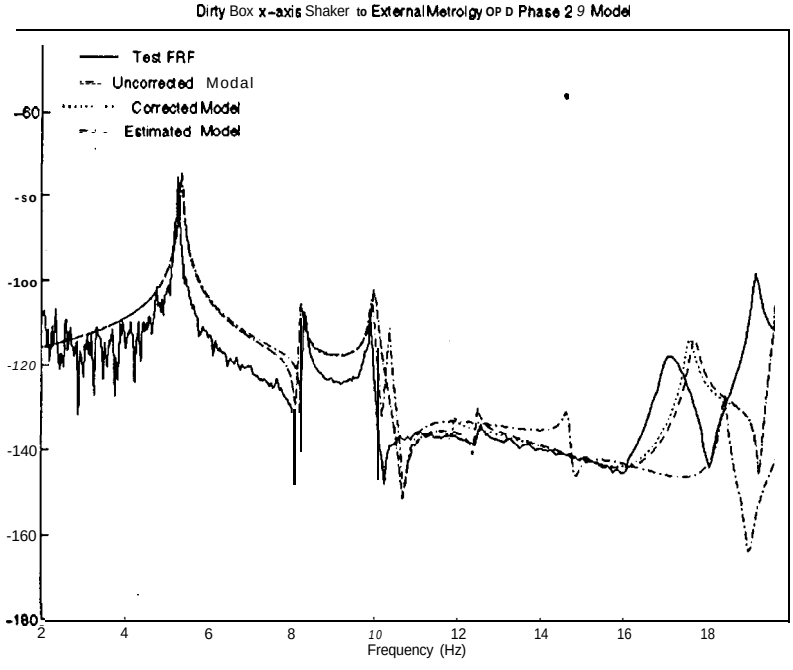

Figure 4-2 Test Validation of the Open-Loop Transfer Function Between the x-axis Dirty Box force Input to the External Metrology OPD.

5. CONCLUSION

A testing and modeling approach has been proposed herein which minimizes costs and schedule impacts for phased assembly of large opto-mechanical structures. An in-situ component testing and identification strategy was implemented on the MPI testbed. The in-situ strategy minimized the impact of the testing on the hardware delivery schedule, by not requiring that the components be tested on separate test fixtures prior to integration with the main structure. Similarly, the cost and complexity of the testing were minimized.

Several mode shape expansion methods have been proposed and investigated, These expansion techniques fall into three main categories. The first one uses direct solutions of the static and

dynamic equations to obtain a closed-form equation. This category includes the Guyan and the Kidder methods. It is shown that these direct methods can also be written in terms of an unconstrained minimization problem. The second category uses least-squares methods to minimize the error between the measured and modeled eigenvectors. Within this category, the Procrustes method imposes orthogonality of the mode shapes. The third category formulates the expansion as a least-squares minimization problem, in which measurement or expansion error is incorporated as a quadratic inequality constraint,

The trade study demonstrated that the LSQI method based on minimization of the dynamic force equation and subject to bounds imposed by measurement noise has the best performance. It is insensitive to moderate amounts of measurement error, and is capable of predicting eigenvectors at unmeasured dofs with greater accuracy than the noise-corrupted data measured at those locations. LSQI is the only method which is capable of regularizing global and local model errors, resulting in mode shapes of higher accuracy than the model originally predicted, even in the presence of experimental noise. It has also been shown on actual data that the LSQI method was the only expansion method capable of locating damaged elements in a model. This makes the LSQI expansion method ideally suited for recursive model updating, damage detection and response prediction technique. A new LSQI algorithm has also been proposed which significantly reduced the computational requirements of conventional LSQI solution techniques.

The Element Modal Strain Energy Error (EMSEE) criteria was used for element error localization, The EMSEE allowed for systematic quantification of the model form and element parameter errors, Use of the LSQI mode shape expansion technique enabled calculation of the EMSEE, Evaluation of the EMSEE for the identified mode shapes resulted in the discovery of several model form errors, both human errors and lack of modeling fidelity in certain elements, The correction of these errors resulted in significant improvement in the model accuracy. Finally, EMSEE was used to target physical parameters for estimation,

Model parameter estimation provided updated physical parameters of components as they were added on, preserving the validity of the previously updated components. The estimation algorithm incorporated a component mode synthesis solution of the eigenvalue problem in order to ease the computational intensity of the algorithm. The previously used Bayesian estimation technique was modified to incorporate a line search algorithm that improved convergence time by several orders of magnitude.

The model updating methodology was developed to be realistically and cost effectively implemented, The estimation algorithm, LSQI modal expansion, and EMSEE calculation were performed on a Sun Sparcstation 10 in MATLAB using IMOS functions.

IMOS was then used to synthesize the structural model with optical and control parameters. Measurements obtained on the MPI testbed demonstrated the accuracy of the integrated model predictions, thus validating the testing and modeling approach recommended herein for complex opto-mechanical structures.

6. ACKNOWLEDGMENTS

This work was performed at the Jet Propulsion Laboratory, California Institute of Technology, under contract with the National Aeronautics and Space Administration. The authors would like to thank R. A. LaSkin and G. B. Neat for the guidance and commitment of resources that made this work possible.

7. REFERENCES

[CRA81]. Craig, R. R. Jr., "Structural Dynamics, an Introduction to Computer Methods", John Wiley & Sons Publ., 1981.

[[FLE87]. Fletcher, R., "Practical Methods of Optimization", Second Edition, John Wiley & Sons Publ., 1987.

[GOL83]. G.H. Golub and C.F. Van Loan, *Matrix Computations*, John Hopkins Univ. Press, Baltimore, MD., 1983.

[GUY65]. R.J., Guyan, "Reduction of Stiffness and Mass Matrices", *AIAA Journal*, Vol. 3, No, 2, 1965.

[HAS91]. Hasselman, T. K., Chrostowski, J. D., and Ross, T. J., "SSID/PDAC (Structural System Identification) Theoretical Manual (Version 1.0)", Technical Report No, TR-91-1152-1, prepared for NASA by Engineering Mechanics Associates, December 1991.

[HUR64]. Hurty, W. C., "Dynamic Analysis of Structural Systems by Component Mode Synthesis", NASA/JPL Technical Report No. 32-530, Jan, 15, 1964.

[KID73]. Kidder, R.L., "Reduction of Structural Frequency Equations", *AIAA Journal*, Vol. 11, No. 6, June, 1973.

[LEV92]. M. B. Levine-West, J. Red-Horse, and E. Marek, "A Systems Approach to High Fidelity Modeling", Proceedings of the 1st Space Microdynamics and Accurate Control Symposium, Nice, France, November 1992,

[LEV94]. Levine-West, M., Kissil, A., and Milman, M., "Evaluation of Mode Shape Expansion Techniques on the Micro-Precision Interferometer Truss", Proc. 12th IMAC, Honolulu, HA, Feb. 1994

[LEV96]. M. B. Levine-West, M. Milman, and A. Kissil, "Mode Shape Expansion Techniques for Prediction: Experimental Evaluation", AIAA Journal, Vol. 34, No. 4, April 1996.

[LEV97]. M. B. Levine-West, M. Milman, and A. Kissil, "Mode Shape Expansion Techniques for Prediction: Analysis", to be submitted to AIAA Journal, 1997.

[MEL96]. J.W. Melody and G.W. Neat, "Integrated Modeling Methodology Validation Using the Micro-Precision Interferometer Testbed", Proc. Of the 1996 Conference on Dicisiona nd control, Kobe, Japan, Dec. 1996.

[MIL97]. M. H. Milman, and M. B. Levine-West, "Integrated Modeling Tools for Precision Multidisciplinary Systems", Proceedings of the 2nd Space Microdynamics and Accurate Control Symposium, Toulouse, France, May 1997.

[NEA97]. G. N. Neat and J. M. Melody, "Control Technology Readiness for Future Spaceborne Interferometer Missions", Proceedings of the 2nd Space Microdynamics and Accurate Control Symposium, Toulouse, France, May 1997.

[PEC96]. N, Peck and S. Wilson, "A Comparison of Four Model Linear. Optimization Updating Schemes for Use in IMOS", JPL Interoffice Memorandum, No. 345-96-050, Jet Propulsion Laboratory, Pasadena, CA, August 8,1996.

[SMI90]. Smith, S. W., and Beattie, C.A., 1990, "Simultaneous Expansion and Orthogonalization of Measured Modes for Structure Identification", Proc. AIAA Dynamics Specialist Conference, Long Beach, Ca., April.

7. REFERENCES

[CRA81]. Craig, R.R. Jr., "Structural Dynamics, an Introduction to Computer Methods", John Wiley & Sons Publ., 1981.

[[FLE87]. Fletcher, R., "Practical Methods of Optimization", Second Edition, John Wiley& Sons Publ., 1987.

[GOL83]. G.H. Golub and C.F. Van Loan, *Matrix Computations,* John Hopkins Univ. Press, Baltimore, MD., 1983.

[GUY65]. R. J., Guyan, "Reduction of Stiffness and Mass Matrices", *AIAA Journal,* Vol. 3, No. 2, 1965.

[HAS91]. Hasselman, T. K., Chrostowski, J. D., and Ross, T. J., "SSID/PDAC (Structural System Identification) Theoretical Manual (Version 1.0)", Technical Report No. TR-91-1152-1, prepared for NASA by Engineering Mechanics Associates, December 1991,

[HUR64]. Hurty, W. C., "Dynamic Analysis of Structural Systems by Component Mode Synthesis", NASA/JPL Technical Report No. 32-530, Jan, 15, 1964.

[KID73]. Kidder, R, L., "Reduction of Structural Frequency Equations", *AIAA Journal,* Vol. 11, No. 6, June, 1973,

[LEV92]. M, B. Levine-West, J. Red-Horse, and E. Marek, "A Systems Approach to High Fidelity Modeling", Proceedings of the 1st Space Microdynamics and Accurate Control Symposium, Nice, France, November 1992,

[LEV94]. Levine-West, M., Kissil, A., and Milman, M., "Evaluation of Mode Shape Expansion Techniques on the Micro-Precision Interferometer Truss", Proc. 12th IMAC, Honolulu, HA, Feb. 1994

[LEV96]. M. B. Levine-West, M. Milman, and A. Kissil, "Mode Shape Expansion Techniques for Prediction: Experimental Evaluation", AIAA Journal, Vol. 34, No. 4, April 1996.

[LEV97]. M. B. Levine-West, M. Milman, and A. Kissil, "Mode Shape Expansion Techniques for Prediction: Analysis", to be submitted to AIAA Journal, 1997.

[MEL96]. J.W. Melody and G. W. Neat, "Integrated Modeling Methodology Validation Using the Micro-Precision Interferometer Testbed", Proc. Of the 1996 Conference on Dicisiona nd control, Kobe, Japan, Dec. 1996,

[MIL97]. M. H. Milman, and M. B. Levine-West, "Integrated Modeling Tools for Precision Multidisciplinary Systems", Proceedings of the 2nd Space Microdynamics and Accurate Control Symposium, Toulouse, France, May 1997.

[NEA97]. G.N. Neat and J. M. Melody, "Control Technology Readiness for Future Spaceborne Interferometer Missions", Proceedings of the 2nd Space Microdynamics and Accurate Control Symposium, Toulouse, France, May 1997.

[PEC96]. N. Peck and S, Wilson, "A Comparison of Four Model Linear Optimization Updating Schemes for Use in IMOS", JPL Interoffice Memorandum, No. 345-96-050, Internal Document, Jet Propulsion Laboratory, Pasadena, CA, August 8, 1996.

SMI90]. Smith, S. W., and Beattie, C. A., 1990, "Simultaneous Expansion and Orthogonalization of Measured Modes for Structure Identification",, Proc. AIAA Dynamics Specialist Conference, Long Beach, Ca., April.